

SUPPLEMENTARY MATERIAL TO  
**Investigation of the adsorption behaviors of thymol blue, crystal violet,  
and rhodamine b on lichen-derived activated carbon**

HÜLYA KOYUNCU<sup>1\*</sup> and ALİ RIZA KUL<sup>2</sup>

<sup>1</sup>Bursa Technical University, Faculty of Engineering and Natural Sciences, Chemical Engineering Department, 16310, Bursa, Türkiye, and <sup>2</sup>Van Yüzüncü Yıl University, Faculty of Science, Chemistry Department, 65080, Van, Türkiye.

Table S-I. Some specifications of TB, CV, and RB

	Thymol Blue	Crystal Violet	Rhodamine B
Molecular structure			
Chemical formula	C <sub>27</sub> H <sub>30</sub> O <sub>5</sub> S	C <sub>25</sub> H <sub>30</sub> ClN <sub>3</sub>	C <sub>28</sub> H <sub>31</sub> ClN <sub>2</sub> O <sub>3</sub>
Molecular weight	466.59 g/mol	407.99 g/mol	479.02 g/mol
GHS pictograms			

\*Corresponding author e-mail: hulya.koyuncu@btu.edu.tr



(a)

(b)

Fig. S-1. a) Lichen *Pseudevernia furfuracea* from Ericek-Bursa; b) lichen-derived activated carbon.

Table S-II. The linearized versions of the PFO, PSO, IDM, Langmuir, Freundlich, and D-R models

Model Name	Model Equation	Plots axis (y ; x)	Model Parameter
PFO	$\ln (q_e - q_t) = \ln (q_e) - k_1 * t$	$\ln(q_e - q_t) ; t$	$q_e, q_t : (\text{mg g}^{-1})$ $k_1 : (\text{min}^{-1})$
PSO	$\frac{t}{q_t} = \frac{1}{k_2 * q_e^2} + \frac{t}{q_e}$ $k_0 = k_2 * q_e^2$	$\frac{t}{q_t} ; t$	$k_2, k_0 : (\text{g mg}^{-1} \text{min}^{-1})$
IDM	$q_t = k_d * t^{1/2} + \theta$	$q_t ; t^{1/2}$	$k_d : (\text{mg g}^{-1} \text{min}^{-1/2})$ $\theta : (\text{mg g}^{-1})$
Langmuir	$\frac{1}{q_e} = \frac{1}{K * C_e * q_m} + \frac{1}{q_m}$	$\frac{1}{q_e} ; \frac{1}{C_e}$	$K : (\text{L mg}^{-1})$ $C_e : (\text{mg L}^{-1})$ $q_m : (\text{mg g}^{-1})$
Freundlich	$\ln (q_e) = \ln (k_f) + \frac{1}{n} * \ln (C_e)$	$\ln(q_e) ; \ln(C_e)$	$k_f : (\text{mg g}^{-1})$
D-R	$\ln (q_e) = \ln (q_m) - K' * \epsilon^2$ $\epsilon = R * T * \ln (1 + 1/C_e)$ $E = 1/\sqrt{2 * K'}$	$\ln (q_e) ; \epsilon^2$	$q_m, q_c : (\text{mol g}^{-1})$ $\epsilon$ : Polanyi potential $K' : (\text{mol}^2 \text{kJ}^{-2})$ $E : (\text{kJ mol}^{-1})$

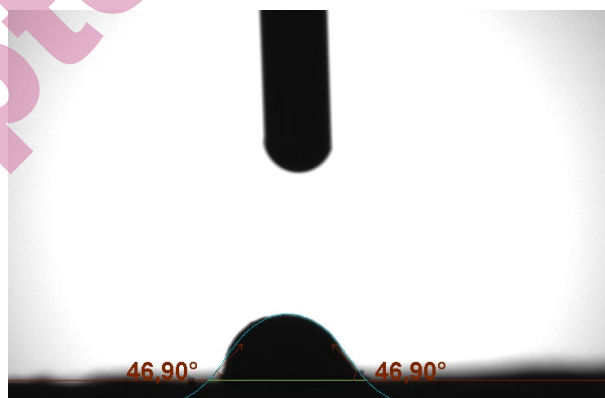


Fig. S-2. Contact angle of the LDAC.

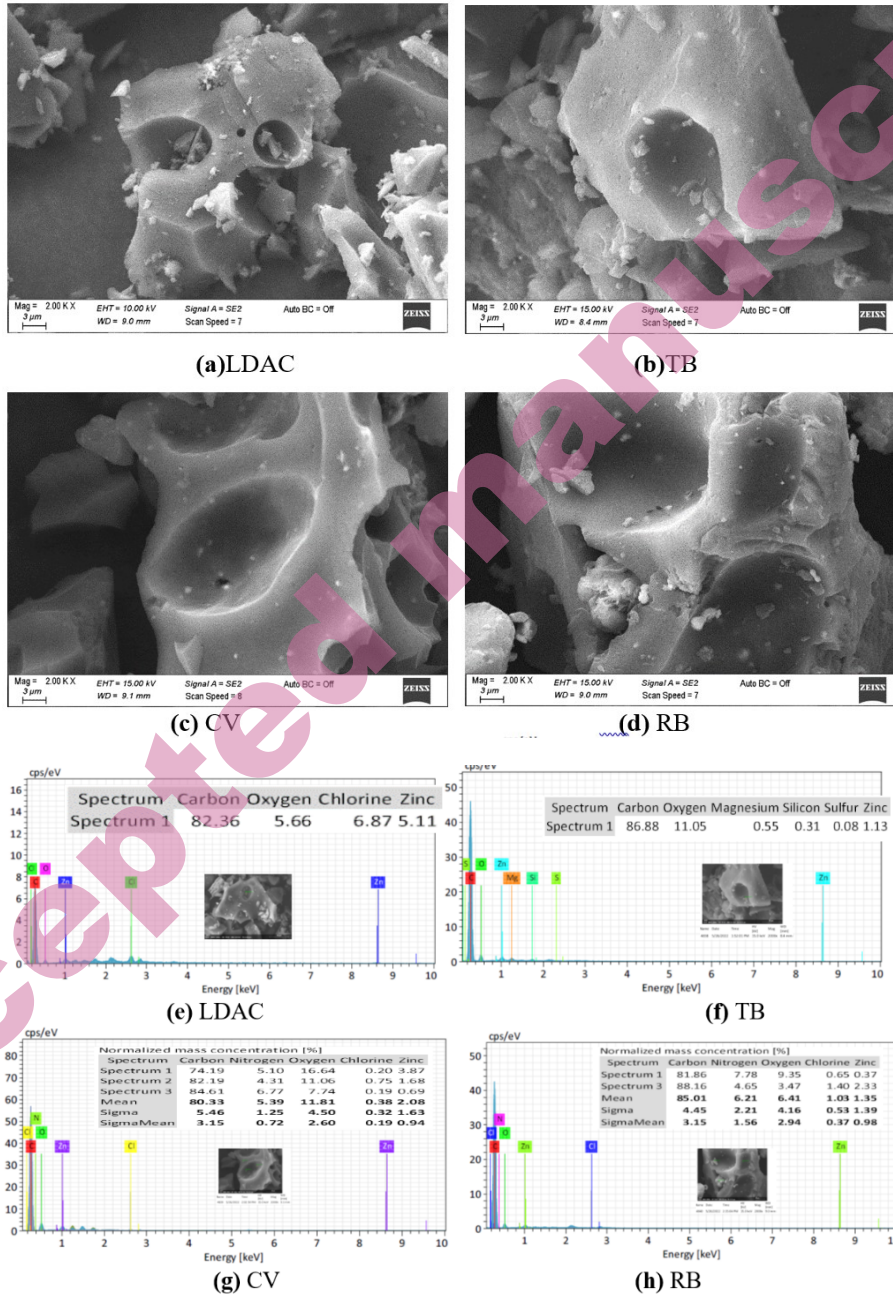


Fig. S-3. SEM photos and EDX results of the LDAC before (a, e) and after TB (b, f), CV (c, g), RB (d, h) loaded.

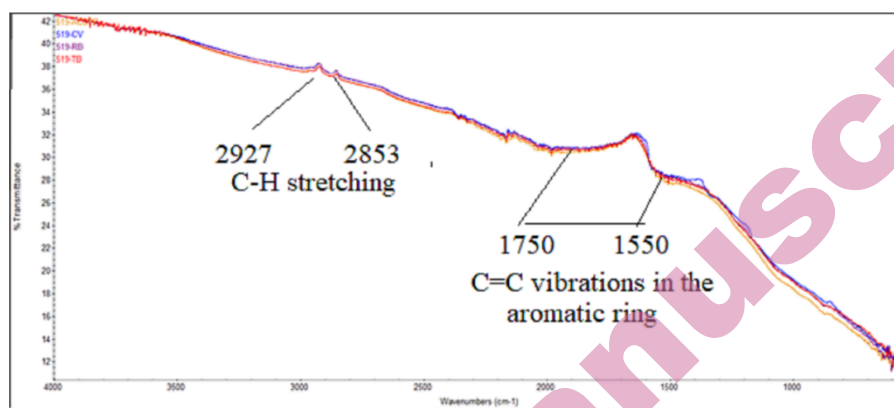


Fig. S-4. FT-IR interferograms of the LDAC before and after TB, CV, and RB loaded.

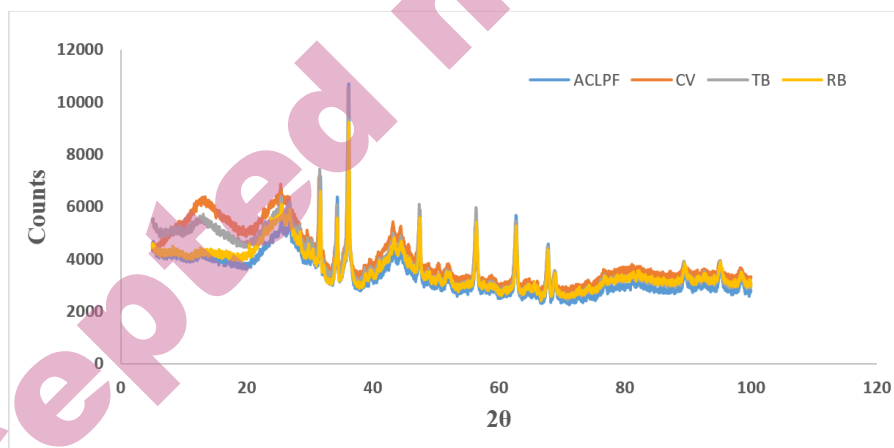


Fig. S-5. XRD patterns of the LDAC before and after TB, CV, and RB adsorptions.

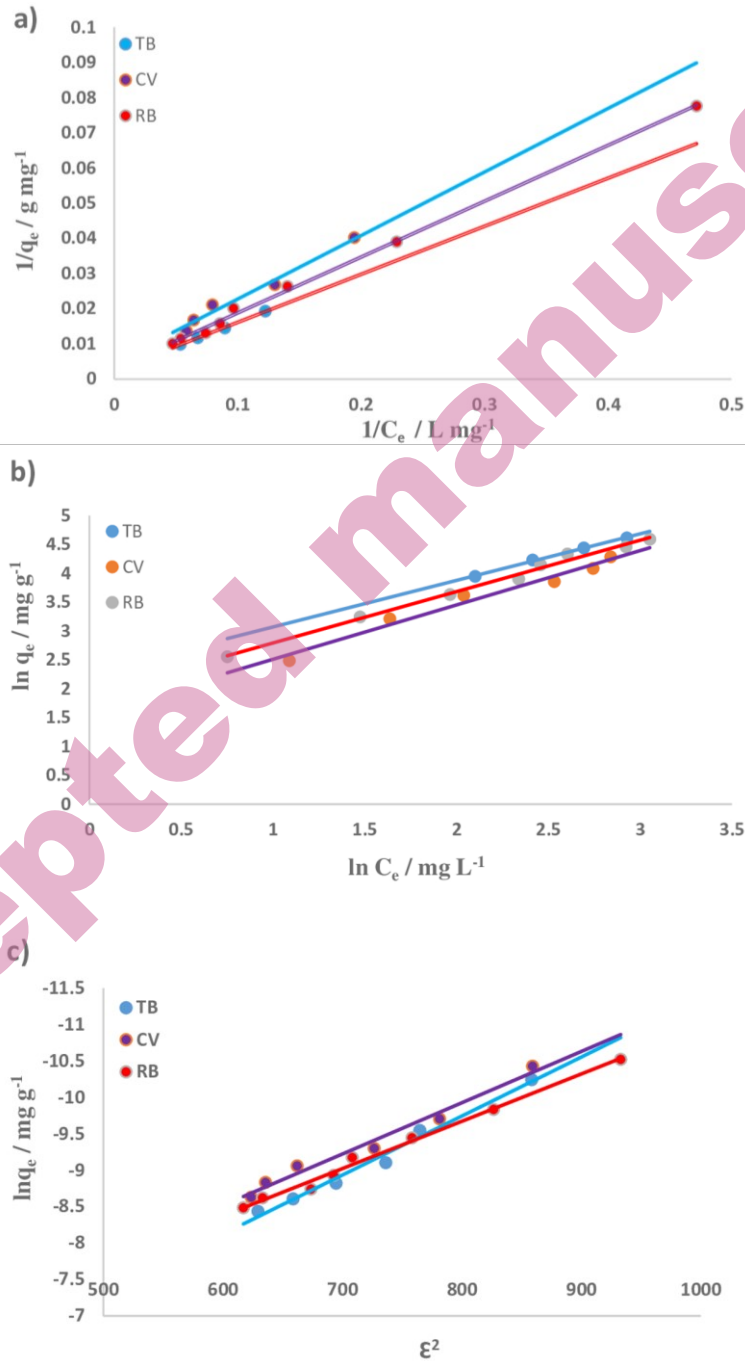


Fig. S-6. a) Langmuir; b) Freundlich; c) D-R isotherms for TB, CV, and RB.

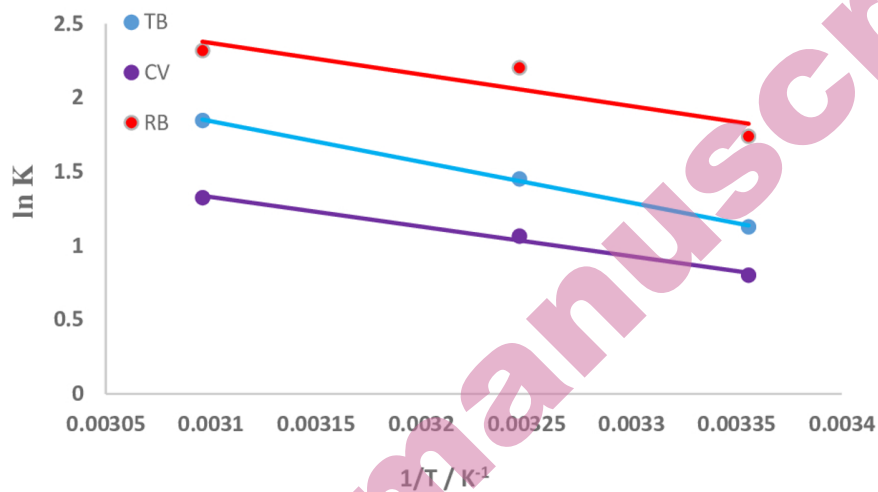


Fig. S-7. The thermodynamic plots for TB, CV, and RB adsorption.

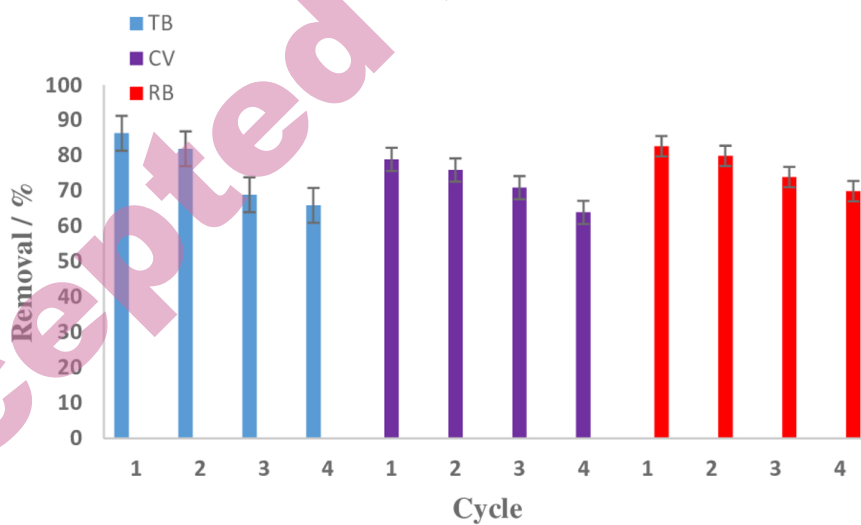


Fig. S-8. The Reusability of the LDAC for TB, CV, and RB adsorption.